Eur. Phys. J. B **11**, 377–383 (1999)

THE EUROPEAN PHYSICAL JOURNAL B

EDP Sciences

Heavy electron $YbNi_2B_2C$ and giant exchange YbNiBC: ^{170}Yb Mössbauer spectroscopy and magnetization studies

P. Bonville[1,a], J.A. Hodges[1], Z. Hossain[2], R. Nagarajan[2], S.K. Dhar[2], L.C. Gupta[2], E. Alleno[3,4], and C. Godart[3,4]

[1] CEA, Centre d'Études de Saclay, Département de Recherche sur l'État Condensé, les Atomes et les Molécules, 91191 Gif-sur-Yvette Cedex, France
[2] Tata Institute of Fundamental Research, Bombay 40005, India
[3] LCMTR-CNRS, Groupe des Laboratoires de Thiais, 2-8 rue Henri-Dunant, 94320 Thiais, France
[4] LURE, Université Paris-Sud, 91405 Orsay Cedex, France

Received 5 February 1999

Abstract. We report low temperature ^{170}Yb Mössbauer spectroscopy and magnetization measurements on two tetragonal non-superconducting quaternary borocarbides, $YbNi_2B_2C$ and YbNiBC, and present L_{III} edge X-ray absorption data in YbNiBC. Both compounds show evidence of $4f$-conduction band hybridisation. In the heavy electron $YbNi_2B_2C$, measurements down to 0.023 K show that only a small hyperfine interaction is present and we estimate an upper limit of 0.05–0.1 μ_B for any Yb moment. In YbNiBC, magnetic ordering is observed below 4.2 K, in agreement with previous specific heat measurements. The single ion easy magnetization axis lies along the **c** axis but the ordered Yb moments lie in the basal (**a**, **b**) plane. Their (extrapolated) saturated value is unusually low (0.35 μ_B). The Yb-Yb exchange interaction is very large and highly anisotropic with the dominant component lying in the basal plane. We also report ^{166}Er Mössbauer and specific heat data in the ferromagnet ErNiBC.

PACS. 74.70.Dd Ternary, quarternary and multinary compounds (including Chevrel phases, borocarbides etc.) – 75.30.Mb Valence fluctuation, Kondo lattice, and heavy-fermion phenomena – 76.80.+y Mössbauer effect; other γ-ray spectroscopy

1 Introduction

The discovery of superconductivity in the quaternary system Y-Ni-B-C [1,2], and the possibility of replacing Y by the magnetic rare earths without destroying superconductivity, has injected new life into the studies of the phenomenon of superconductivity and its interplay with long range magnetic order. The quaternary magnetic superconductors RNi_2B_2C (R = Y, rare earth) [3,4] are particularly interesting [5]: they show relatively high superconducting transition temperatures T_c and Néel temperatures T_N and the relative magnitude of T_c and T_N may be varied by changing the rare earth ($T_c > T_N$ in $ErNi_2B_2C$ and in $TmNi_2B_2C$, $T_c < T_N$ in $DyNi_2B_2C$ and $T_c \approx T_N$ in $HoNi_2B_2C$). In this context the properties of the member corresponding to the end magnetic element of rare earth series, $YbNi_2B_2C$, are of great interest.

Magnetic susceptibility measurements in $YbNi_2B_2C$ show that, above 100 K, the effective paramagnetic Yb moment is nearly equal to that of the free trivalent Yb ion [6,7]. On the basis of the pattern of T_c and T_N in the RNi_2B_2C series of superconductors, one would expect $YbNi_2B_2C$ to be a magnetic superconductor with a T_c of about 12 K and $T_N < T_c$. No superconducting transition has, however, been observed down to 0.6 K, showing there is an anomalous suppression of T_c for this compound [6,7]. At low temperatures, the magnetic susceptibility deviates from a Curie-Weiss behaviour, below 50 K a large drop in resistivity occurs and a heavy fermion state (a narrow f-band) evolves [6,7] transferring the entropy associated with magnetic degrees of freedom to the itinerant states. The presence of a strong hybridisation of conduction electrons with $4f$ electrons is indicated by the large negative paramagnetic Curie temperature: $\theta_p \simeq -100$ K, and is further confirmed by the fact that the substitution of only 0.1 atomic fraction of Y by Yb in YNi_2B_2C depresses T_c ($\sim$ 15.5 K) by about 13 K [8]. This is the largest known T_c suppression due to Yb substitution.

In the quaternary borocarbide YbNiBC [9] a contrasting scenario takes place. This material has a structure related to that of $YbNi_2B_2C$ [10,6], with two Yb-C layers separating the Ni_2B_2 layer. Magnetic measurements show that in this material, the Yb ions undergo a magnetic transition (T_N) at about 4.2 K [9] which is an unusually high value among the known Yb-based magnetically ordered materials. That T_N is anomalously high also follows from the consideration of the T_N of the other members of the RNiBC series. For instance, considering that T_N

[a] e-mail: bonville@spec.saclay.cea.fr

of GdNiBC is 14 K [11,9], then, according to the de Gennes scaling, T_N of YbNiBC should only be ~ 0.3 K. In addition, the value of the paramagnetic Curie temperature is large and negative ($\theta_p \sim -40$ K) [9]. These features suggest the presence in YbNiBC of a modest hybridisation of the $4f$ Yb electrons with conduction electrons, *i.e.* of a partial delocalisation of the former.

The two materials are therefore Kondo lattices, containing almost trivalent hybridised Yb ions. In the case of $YbNi_2B_2C$, a rather strong delocalisation of the Yb $4f$ electrons leads to a nonmagnetic ground state whereas a partial delocalisation of the Yb $4f$ electrons in YbNiBC leads to an anomalously high magnetic ordering temperature. In this light, we undertook the ^{170}Yb Mössbauer studies of these two materials so as to obtain microscopic information about the magnetic moment of the Yb ions. We point out here that most of the known heavy fermion compounds are Ce- or U-based intermetallics, both of which are not suitable for Mössbauer/NMR investigations. This is another important aspect of the present studies.

We also present data in ErNiBC, which is isostructural to YbNiBC, and where, as usual, the trivalent Er ions show no hybridisation. While the magnetic ordering temperature of ErNiBC ($T_C \sim 4$ K) is almost the same as that of YbNiBC, the former compound orders ferromagnetically [12] whereas the latter appears to order antiferromagnetically [9].

2 Experimental

The materials $YbNi_2B_2C$ and YbNiBC were prepared as described in references [6,9]. ErNiBC was prepared by conventional arc melting technique. The magnetisation measurements were carried out around 2 K using a commercial SQUID magnetometer. Heat capacity measurements were carried out using a home built apparatus based on a semi-adiabatic heat pulse technique. The L_{III} edge X-ray absorption study was performed at the LURE synchrotron facility (Orsay, France).

The Mössbauer transition for both isotopes ^{170}Yb ($E_0 = 84.3$ keV) and ^{166}Er ($E_0 = 80.6$ keV) links the ground nuclear state with $I_g = 0$ to the first excited nuclear state with $I = 2$. The monochromatic γ-ray source is neutron irradiated Tm^*B_{12} for ^{170}Yb and $Ho^*_{0.4}Y_{0.6}H_2$ for ^{166}Er. The absorption spectra were recorded using an electromagnetic drive with a triangular velocity signal. The velocity to frequency conversion ratios are: 1 mm/s = 68 MHz for ^{170}Yb and 1 mm/s = 65 MHz for ^{166}Er. The spectra below 1.4 K were recorded in a home built ^{3}He-^{4}He dilution refrigerator.

3 Mössbauer and magnetization data in $YbNi_2B_2C$

The Yb ion in $YbNi_2B_2C$ is very close to trivalent, as evidenced by the L_{III} edge X-ray absorption, and the thermal variation of the susceptibility above 100 K. Below this temperature, deviations occur relative to a Curie-Weiss law [6]. Because the Sommerfeld coefficient of the specific heat is rather large as in heavy electron systems, the absence of magnetic ordering down to 2 K [6] was assigned to the presence of Kondo spin fluctuations. However, it is possible that a magnetically ordered or correlated state, with small moments, could exist at very low temperature as found in some other heavy electron compounds [13,14].

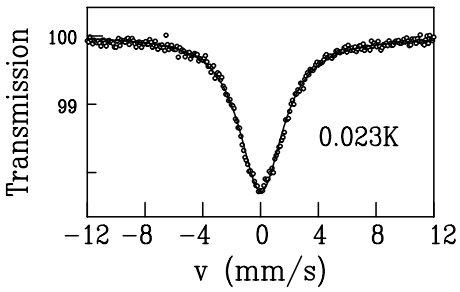

Fig. 1. ^{170}Yb Mössbauer absorption spectrum at 0.023 K in $YbNi_2B_2C$. The solid line is a fit to a Lorentzian line shape.

The ^{170}Yb Mössbauer absorption spectra were recorded at 0.023 K, 0.2 K, 0.5 K and 4.2 K, the Tm^*B_{12} γ-ray source having a Lorentzian line shape with full width at half-maximum (FWHM) $G = 2.9(1)$ mm/s. In $YbNi_2B_2C$, the spectra show a single line in the studied temperature range (0.023 K–4.2 K). From 0.023 K (see Fig. 1) to 0.5 K, the FWHM is $G = 3.75(5)$ mm/s, slightly larger than the source line width; at 4.2 K, it is somewhat broader: $G = 3.90(5)$ mm/s. In the whole temperature range, the line shape is not perfectly Lorentzian, indicating the presence of a small hyperfine interaction which can be either of quadrupolar or of magnetic origin (or both). However, it is not likely that a (small) magnetic hyperfine field is present at 4.2 K. Therefore, as a hypothesis, we think that the broadening at 4.2 K can be mainly of dynamic origin, *i.e.* due to electronic spin fluctuations. At the lowest temperatures, the broadening could be interpreted as the presence of a small hyperfine field, of magnitude $\simeq 12$ T, which corresponds to a Yb^{3+} $4f$ shell moment of 0.12 μ_B (for $^{170}Yb^{3+}$, 1 μ_B gives rise to a hyperfine field of 102 T). In fact, taking into account the possible contribution of a quadrupolar interaction at the Yb site with tetragonal symmetry, we suggest the upper limit of any ordered moment is 0.05–0.1 μ_B. The presence or absence of small magnetic moments in $YbNi_2B_2C$ could be checked by a technique like positive muon spectroscopy, which may be able to detect moments as low as 0.01 μ_B.

The magnetization data in applied fields up to 5 T is shown in Figure 2 (open squares). It shows a slight curvature at low fields, with a rather small polarization of $\simeq 0.5$ μ_B per Yb^{3+} ion at the maximum field of 5 T. This behaviour is typical for Kondo lattices with a Kondo temperature of a few 10 K.

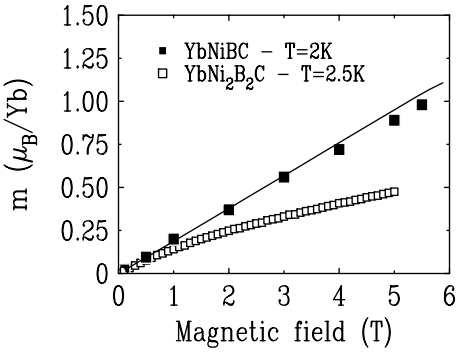

Fig. 2. Isothermal magnetization curves at 2 K in YbNiBC (filled squares) and at 2.5 K in $YbNi_2B_2C$ (open squares). The solid line is a self-consistent calculation of the magnetization for YbNiBC, within a Kramers doublet with anisotropic g-tensor and molecular field tensor (see text).

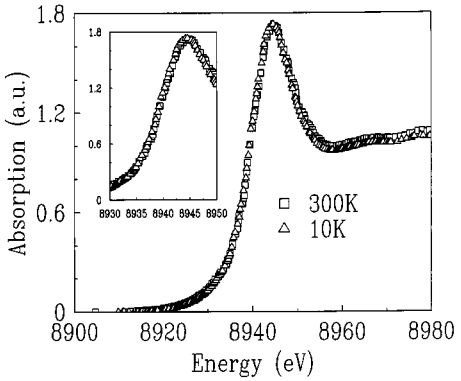

Fig. 3. L_{III} edge X-ray absorption spectrum *vs.* energy in YbNiBC at 10 K and 300 K. The inset is a magnified view of the low energy part of the absorption spectra and shows that no structure is observed near 8935 eV which would correspond to Yb^{2+}.

4 Experimental results, crystal field and giant Yb-Yb exchange in YbNiBC

4.1 Crystal structure and L_{III} edge X-ray absorption data

The major lines of the X-ray diffraction pattern of our YbNiBC sample belong to the tetragonal LuNiBC-type structure. Four impurity lines correspond to $YbNi_2B_2C$, with a maximum intensity of 6% of the strongest YbNiBC line. The L_{III} absorption edge spectra at 10 K and 300 K are shown in Figure 3. The main peak around 8943 eV corresponds to Yb^{3+}; no contribution of Yb^{2+} (at $\simeq$ 8935 eV) is observed as shown in the insert. The absorption profiles at 10 K and 300 K are identical, showing that the Yb ion is trivalent in the whole temperature range. The half width at half maximum ($\sim$ 4.8 eV) is slightly larger than that expected from the hole lifetime ($\sim$ 4 eV). This could correspond to the presence of a small amount of a Yb^{3+} containing impurity, having a small chemical shift relatively to YbNiBC; this could be $YbNi_2B_2C$, detected in the X-ray diffractogram, and/or the oxide Yb_2O_3, due to surface oxidation of the powder sample.

4.2 The Mössbauer and magnetization data

The specific heat of YbNiBC shows a well defined anomaly close to 4 K, indicating the existence of magnetic ordering, and the magnetic susceptibility data suggest an antiferromagnetic order at 4 K [9]. The ^{170}Yb Mössbauer absorption spectra in the temperature range 4.25 K $\leq T \leq$ 60 K can be very well accounted for using the axially symmetric quadrupolar hyperfine Hamiltonian in the excited nuclear state:

$$\mathcal{H}_Q = \alpha_Q \left[I_z^2 - \frac{I(I+1)}{3} \right], \qquad (1)$$

where α_Q is the quadrupolar hyperfine coupling parameter, which is proportional to the z-component of the electric field gradient (EFG) tensor V_{ij} at the rare earth site: $\alpha_Q = \frac{eQV_{zz}}{8}$, Q being the quadrupole moment of the $I = 2$ excited nuclear state. The observation of an axially symmetric quadrupolar pattern is in agreement with the tetragonal point symmetry of the Yb site; furthermore, for symmetry reasons, the principal axis of the EFG tensor must be the tetragonal crystallographic **c** axis. Neglecting the possible small contribution to the EFG tensor coming from the lattice charges, the main contribution to α_Q comes from the $4f$-shell electrons, and it is proportional to the $4f$ electron quadrupolar moment Q_{zz}: $\alpha_Q^{4f} = B_Q Q_{zz}$, with $B_Q = 0.276$ mm/s for ^{170}Yb [15]. The low temperature α_Q value therefore yields information on the crystal electric field (CEF) ground wave function of the Yb^{3+} ion and the thermal variation $\alpha_Q(T)$ reflects the progressive population of the crystal field levels as temperature increases. We obtain: $\alpha_Q(4.25\ \text{K}) = 3.65(5)$ mm/s and $\alpha_Q(60\ \text{K}) = 3.55(5)$ mm/s, *i.e.* the thermal variation of α_Q is very weak indicating that the first excited crystal field state lies at an energy higher than about 150 K from the ground state (provided there is no excited state with a quadrupole moment close to that of the ground state).

As the temperature is lowered below 4.25 K, the spectra show modest but clearly visible changes (see Fig. 4) and they can no longer be fitted using the quadrupole hyperfine interaction (1) alone. To obtain satisfactory linefits, we need to introduce a small hyperfine field $\mathbf{H}_{\rm hf}$ perpendicular to the principal axis of the EFG tensor (for instance along a direction x in the (**a**, **b**) plane), and the corresponding hyperfine Hamiltonian is:

$$\mathcal{H}_{\rm hf} = \alpha_Q \left[I_z^2 - \frac{I(I+1)}{3} \right] - g_{\rm n}\mu_{\rm n} H_{\rm hf} I_x, \qquad (2)$$

where $g_{\rm n}\mu_{\rm n}$ is the gyromagnetic ratio of the excited nuclear state. When the magnetic hyperfine interaction is much smaller than the quadrupolar interaction, a perturbation treatment of the former with respect to the latter, which has eigenstates $|I_z = 0\rangle$, $|I_z = \pm 1\rangle$ and $|I_z = \pm 2\rangle$ in the $\{\text{I} = 2\}$ multiplet, shows that there are no line shifts to first order perturbation when the hyperfine field is perpendicular to the principal axis of the EFG tensor. A small transverse hyperfine field has therefore only a small spectral effect, which explains the minor modifications as one

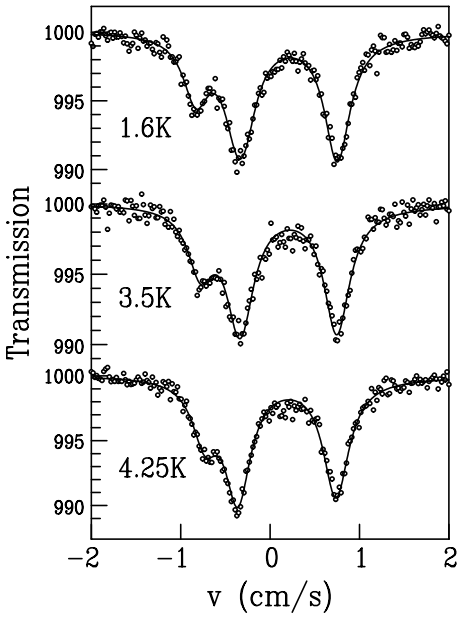

Fig. 4. ^{170}Yb Mössbauer absorption spectra in YbNiBC at selected temperatures. The solid lines are fits to a quadrupolar hyperfine Hamiltonian alone at 4.25 K, and to a quadrupolar Hamiltonian to which is added a magnetic interaction with a small hyperfine field perpendicular to the principal axis of the EFG tensor at 3.5 K and 1.6 K.

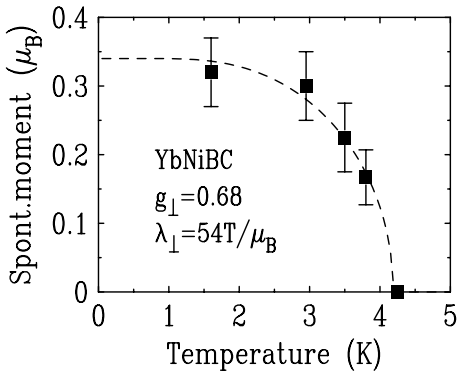

Fig. 5. Thermal variation of the Yb^{3+} spontaneous moment in YbNiBC derived from the hyperfine field values. The dashed line is a S = 1/2 mean field law with $g_\perp = 0.68$ and $\lambda_\perp = -54$ T/μ_B (see text).

enters the magnetically ordered phase in YbNiBC below 4.2 K. Therefore, identifying the principal axis of the EFG tensor with the tetragonal **c** axis, the magnetic structure of YbNiBC is such that the moments are perpendicular to the tetragonal axis. The hyperfine field value at the lowest temperature (1.6 K) is 32.5(4.5) T. This corresponds to a spontaneous magnetic moment of 0.32(5) μ_B per Yb ion. The thermal variation of the spontaneous moment, derived from that of the hyperfine field, is represented in Figure 5. It follows a mean field law for S=1/2 (dashed line in Fig. 5) as will be discussed in Section 4.3, with a saturated spontaneous moment of $\simeq$ 0.35 μ_B. YbNiBC thus contains Yb^{3+} ions having a relatively high magnetic ordering temperature with a relatively low spontaneous magnetic moment, which suggests a giant exchange coupling among the Yb ions. Let us remark that a similar situation occurs in the orthorhombic ferromagnet YbNiSn [16], which also has a high magnetic transition temperature (T_c = 5.65 K) along with a small spontaneous moment (0.85 μ_B).

The magnetization data at 2 K in YbNiBC are shown in Figure 2 (full squares). It is linear with the field and shows no hint of any curvature up to 5.5 T. The magnetization curve in the paramagnetic phase, at 7 K, is practically identical to that at 2 K.

The results of the heat capacity measurements [9] near the magnetic transition show an interesting feature. The magnetic entropy associated with magnetic ordering of the Yb ions (for estimating the magnetic entropy, the lattice and conduction electron contributions were taken to be the same as in LuNiBC) attains a value of about 2.5 J mol^{-1} K^{-1} at the transition temperature (taken as the peak of the heat capacity plot) and approaches the value $R\ln 2$, the theoretical value for a doublet ground state, only near 18 K. The reduction of the entropy released at the magnetic transition with respect to that associated with a doublet can be due either to the presence of short range order above T_N or to the presence of hybridisation of the $4f$ electrons with conduction electrons. In the latter case, it is due to the N-electron Kondo singlet ground state, which prevents the single ion paramagnetic degrees of freedom from being recovered entirely at the magnetic transition. In YbNiBC, we think the reduced entropy release at T_N is caused mainly by hybridisation.

4.3 Interpretation in terms of strong crystal field and exchange anisotropy

To obtain information about the crystal field and exchange interactions, we will analyse the results with a "crystal field only" model and neglect the (probably small) hybridisation of the Yb $4f$ electrons of YbNiBC with conduction electrons. In a tetragonal crystal field, the 8-fold degenerate $J = 7/2$ ground spin-orbit multiplet of the Yb^{3+} ion splits into 4 Kramers doublets [17], whose wavefunctions are of two types: a cubic Γ_7-derived type

$$|\psi_1\rangle = a|J_z = 5/2\rangle + b|J_z = -3/2\rangle, \quad a^2 + b^2 = 1, \quad (3)$$

and its Kramers conjugate, and a cubic Γ_6-derived type

$$|\psi_2\rangle = c|J_z = 7/2\rangle + d|J_z = -1/2\rangle, \quad c^2 + d^2 = 1, \quad (4)$$

and its Kramers conjugate.

We find that the ground state in YbNiBC must be of type $|\psi_2\rangle$ because only this type has a large positive α_Q value as is found experimentally. This large and positive α_Q value corresponds to a large and positive $4f$ shell quadrupole moment. The components $g_z(g_c)$ and $g_\perp$ of the electronic g-tensor as well as α_Q (assumed to be due only to the $4f$ shell) are univocal functions of the coefficients in $|\psi_2\rangle$. Then, starting from the experimental value $\alpha_Q(T = 0) \simeq 3.65$ mm/s, we find: $c = 0.90 \pm 0.02$

and $d = 0.44 \pm 0.03$ and for the ground state g-tensor: $g_z \simeq 6$ and $g_\perp \simeq 0.9$. Alternatively, starting from an extrapolated value of the saturated spontaneous moment $m_\perp(T=0) \simeq 0.35\,\mu_B$, *i.e.* $g_\perp \simeq 0.7$ (the moments are perpendicular to the tetragonal axis), we find $\alpha_Q^{4f} \simeq 4$ mm/s and $g_z \simeq 6.3$. This 10% larger value of α_Q^{4f} with respect to the measured value can be understood if one assumes the presence of a small negative lattice contribution to the EFG tensor. This crystal field only analysis thus shows that the ground state g-tensor is strongly anisotropic ($g_z \sim 6$, $g_\perp \simeq 0.7$, *i.e.* $g_\perp/g_z \simeq 0.12$). The single ion easy magnetic axis is thus the **c** axis. As the magnetic moments in the magnetically ordered phase are perpendicular to the **c** axis, the exchange interaction must be also strongly anisotropic with a principal plane perpendicular to the **c** axis. Such opposite anisotropies of the g-tensor and of the exchange tensor have been observed in the ferromagnet YbNiSn [16]. Within the molecular field approximation, we model the exchange coupling within the ground crystal field doublet by a two-component molecular field constant tensor $\{\lambda_z, \lambda_\perp\}$. Using a self-consistent two-sublattice calculation, we calculated both the thermal variation of the spontaneous moment, which depends on $g_\perp$ and $\lambda_\perp$, and the field variation of the magnetization in the antiferromagnetic phase for a powder sample, which depends on both components of the two tensors. We neglect here the quantum mixing of excited states into the ground state by the Zeeman and/or exchange interaction. This is a valid approximation when the first CEF excited state lies at an energy larger than 150 K from the ground state, as is suggested by the thermal variation of α_Q.

The dashed line in Figure 5, which reproduces the experimental data quite well, is a mean field law obtained with $g_\perp = 0.68$ and $|\lambda_\perp| = 54$ T/μ_B. This huge molecular field constant is necessary in order to explain the relatively high ordering temperature ($T_N \simeq 4.2$ K) with magnetic moments perpendicular to the easy magnetic axis. In order to reproduce the isothermal magnetization curve at 2 K, which, rather unexpectedly, is linear with increasing field, we imposed the previously determined value for the transverse antiferromagnetic molecular field constant ($\lambda_\perp = -54$ T/μ_B) and we fitted λ_z and the ratio $g_\perp/g_z$. The linear variation with the correct slope (Fig. 2) is obtained with the values $\lambda_z = -0.9$ T/μ_B and $g_\perp/g_z = 0.13$. We find the slope is rather independent of the exact g_z value. Thus the exchange interaction tensor in YbNiBC is extremely anisotropic, with $\lambda_z/\lambda_\perp \simeq 0.017$. The calculated magnetization curve at 7 K is practically identical with that at 2 K, in agreement with experiment.

Using the above derived parameters, the magnetic energy $E_i = -\lambda_i(g_i\mu_B)^2/4$ along a direction i can be estimated. One obtains a reliable value for $E_\perp$ (-4.2 K, $|E_\perp| = T_N$), but a less precise value for E_z, due to the uncertainties concerning g_z and λ_z. The E_z value is however close to $E_\perp$, showing that a delicate balance between the anisotropies of the crystal field and exchange interactions is at play to achieve the actual situation with the magnetic moments perpendicular to the tetragonal axis. Furthermore, the presence of $4f$-conduction electron hybridisation, which can lead to a reduction of the crystal field magnetic moment, and the quantum mixing with excited crystal field states, have been neglected. The values derived here for the g- and λ-tensors must therefore be considered as first approximations; our main conclusion, that YbNiBC has a very anisotropic exchange with a giant value in the plane perpendicular to the tetragonal axis, and a ground CEF Kramers doublet with a large anisotropy along the tetragonal axis, remains unchanged.

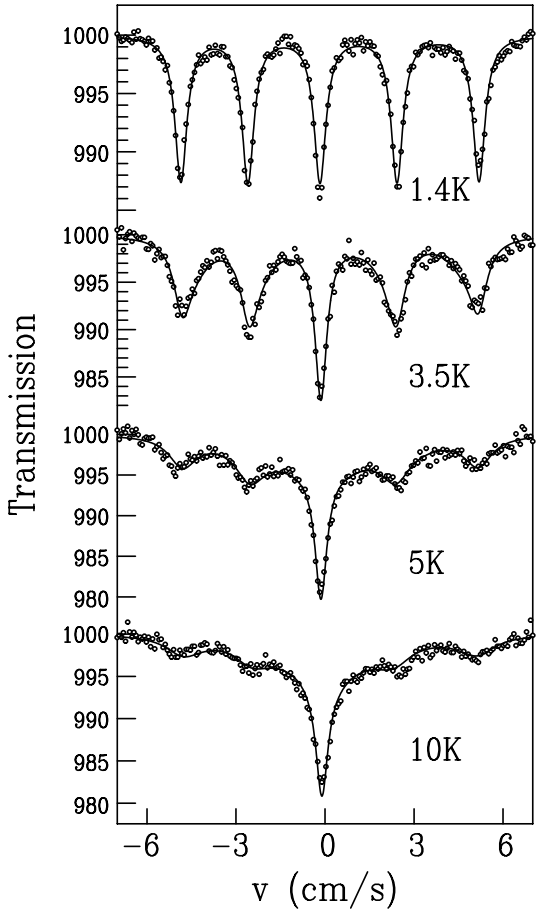

Fig. 6. ^{166}Er Mössbauer absorption spectra in ErNiBC below ($T = 1.4$ K and 3.5 K) and above ($T = 5$ K and 10 K) the Curie temperature $T_C = 4.5$ K. The solid lines are fits to a line shape involving two close lying Kramers doublets (see text).

5 ^{166}Er Mössbauer and specific heat results in ErNiBC

The alloy ErNiBC, isostructural with YbNiBC, has been found to order ferromagnetically below $T_C \simeq 4.5$ K by neutron diffraction measurements [12], with the saturated Er^{3+} magnetic moments of 6.6 μ_B aligned along the tetragonal **c** axis. Mössbauer absorption spectra on the isotope ^{166}Er in ErNiBC at selected temperatures are shown in Figure 6. The spectra show a five line magnetic hyperfine pattern, with line broadening increasing as temperature increases and an overall line splitting showing

only a slight decrease as temperature increases. Furthermore, no spectral anomaly marks the crossing of the Curie temperature (4.5 K), which contrasts with the situation in the antiferromagnetic borocarbide $ErNi_2B_2C$ [18]. The absence of an anomaly at T_C is characteristic of Mössbauer line shapes near the "slow electronic relaxation" limit, *i.e.* the description of the spectra is based on the static axial electronuclear hyperfine Hamiltonian:

$$\mathcal{H}_{\rm hf} = A_z I_z S'_z + \alpha_Q \left[I_z^2 - \frac{I(I+1)}{3} \right], \qquad (5)$$

where S'_z is the z-component of the $S' = 1/2$ effective spin of the ground crystal field Kramers doublet and A_z is the z-component of the magnetic hyperfine tensor, proportional to the electronic g-tensor (for $^{166}Er^{3+}$, and expressing A_z in mm/s: $A_z/g_z \simeq 3.2$). Magnetic fluctuations can occur between the two components of the $S' = 1/2$ ground state, and they are "slow" when the electronic fluctuation rate $1/T_1$ is smaller than the hyperfine Larmor frequency corresponding to $^{166}Er^{3+}$: $\nu_L \simeq 1$ GHz.

The spectrum at 1.4 K can be fitted to Hamiltonian (5) with very slow electronic fluctuations ($1/T_1 \ll \nu_L$), and yields: $A_z \simeq 50$ mm/s and $\alpha_Q \simeq 0.85$ mm/s. This shows that the ground Er^{3+} doublet has $g_z \simeq 15.6$, and hence a saturated moment along the z axis, identified with the tetragonal **c** axis, of $m_0 \simeq 7.7\ \mu_B$. This value, which is higher than that derived from the neutron diffraction data (6.6 μ_B), is close to the value associated with the extremely anisotropic doublet $|J = 15/2;\ J_z = \pm 13/2\rangle$ (7.8 μ_B), but could also correspond to the moment of the state $|J = 15/2;\ J_z = \pm 11/2\rangle$ (6.6 μ_B) if the (negative) conduction electron polarisation is sizeable at the rare earth site. The doublet $|J = 15/2;\ J_z = \pm 15/2\rangle$ has a higher moment of 9 μ_B. The measured α_Q value also is close to those corresponding to the above mentioned first two doublets. It is however probable that the exact wave functions of the Er^{3+} ion are not pure eigenstates of J_z, but contain small admixtures of other states.

As temperature increases, the line broadenings increase relatively rapidly, and this is attributed to a dynamical effect linked with the increase of the electronic fluctuation rate. Attempts to fit the spectral shapes for $T > 1.4$ K with a relaxation line shape within a single Kramers doublet [19] succeed up to 4.2 K but fail to reproduce the shapes of the spectra at higher temperature. Above 4.2 K, acceptable fits can only be obtained by introducing two subspectra. With the reasonable assumption that the Er^{3+} occupies only one crystallographic site (there are local inhomogeneities due, for example, to carbon vacancies, but their concentration is small and they cannot be detected in the X-ray diffractogram), we consider the two components to arise from two closely spaced Kramers doublets. A dynamical line shape involving two such doublets was therefore used to fit the spectra in the whole temperature range (solid lines in Fig. 6). Although good fits can be obtained with various sets of parameters, we find the first crystal field excited doublet must lie within a few Kelvin above the ground state in order to obtain consistent fits in the whole temperature range.

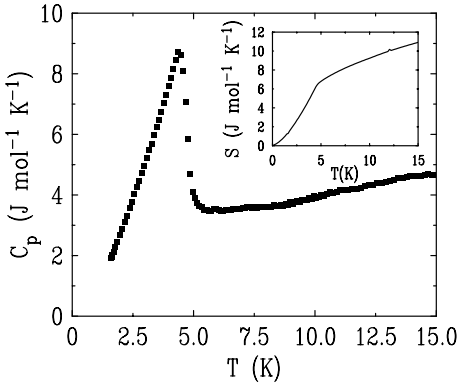

Fig. 7. Thermal variation of the specific heat of ErNiBC. Inset: thermal variation of the magnetic entropy.

The ^{166}Er Mössbauer data in ErNiBC thus show that the ground crystal field state of the Er^{3+} ion is close to $|J = 15/2;\ J_z = \pm 13/2\rangle$ or to $|J = 15/2;\ J_z = \pm 11/2\rangle$ and suggest that the first excited doublet is very close to the ground state.

Our heat capacity data of ErNiBC tend to support this conclusion. A huge anomaly with a peak at 4.25 K and with a height of nearly 9 J mol^{-1} K^{-1} signals the transition to the magnetically ordered state (Fig. 7). The entropy associated with the magnetic transition was estimated by assuming that the phonon and background conduction electron band contributions to the heat capacity in ErNiBC are the same as those observed in LuNiBC (the data on the latter compound have been taken up to 15 K only). For the purpose of estimating the magnetic entropy, below the lowest temperature data point of 1.5 K, the heat capacity plot was smoothly extrapolated to $T = 0$ K. This is a reasonable procedure, as this may result in error in the entropy value of only a few percent. The entropy at the peak thus estimated is 6 J mol^{-1} K^{-1} (inset of Fig. 7). This value already exceeds the theoretical value of $R\ln 2$ (5.76 J mol^{-1} K^{-1}) for a doublet. Further, the entropy increases very sharply in the paramagnetic regime above T_N, and attains a value of nearly 11 J mol^{-1} K^{-1} at 15 K. An entropy release of this magnitude can be ascribed to two closely spaced crystal field doublets, for which the theoretical value is $R\ln 4$ (11.52 J mol^{-1} K^{-1}). Therefore, the heat capacity result supports the conclusion derived from Mössbauer spectroscopy that in ErNiBC the first excited state is separated by less than 10 K from the ground state.

Magnetization measurements at 2 K in fields up to 2 T show a rapid increase of the magnetization followed by a quasi saturation above 1 T, to a value $\simeq 3.5\ \mu_B$ per Er^{3+} ion. This is slightly lower than the value $m_0/2 = 3.85\ \mu_B$ expected for the magnetization of a polycrystalline sample with an Ising-like ground doublet with moment $m_0 \simeq 7.7\ \mu_B$, as derived above. The lower measured value could be due to the influence of the first excited state close to the ground state.

6 Conclusions

The two Yb-based borocarbides studied here, $YbNi_2B_2C$ and YbNiBC, present a common feature, *i.e.* the occurrence of a small magnetic moment (or possibly a vanishing moment in $YbNi_2B_2C$) at low temperature. The small moment can arise due to both $4f$ electron – band electron hybridization and crystal electric field effects; however, the extent of hybridization and its effect are different in the two cases. The magnetic behaviour in these systems fits into the general scheme of Doniach's Kondo-necklace model [20].

In $YbNi_2B_2C$, our ^{170}Yb Mössbauer spectroscopy results show that the magnetic moment on the Yb ion is absent or is less than 0.05–0.1 μ_B down to 0.023 K. In this case, the Kondo coupling is rather strong; strong enough to fully compensate the local moment on the Yb ions and to prevent the onset of magnetic order. Evolution of the heavy fermion state in this material [6] is a natural consequence of this loss of magnetization. In this respect this system behaves like the well-known system $CeRu_2Si_2$ [21]. We note that the measurements reported here are one of a few made down to very low temperatures (0.023 K) which directly show the non magnetic state of the hybridized electrons. The absence of any sizeable quadrupolar hyperfine interaction in this compound, where the Yb ion lies at a site with tetragonal symmetry, is quite surprising. The $T = 0$ K $4f$ quadrupole moment can be strongly reduced in the presence of hybridisation [22], and in addition it could be further screened by the lattice contribution to the EFG, which is generally of a sign opposite to that of the $4f$ contribution.

In YbNiBC, our ^{170}Yb Mössbauer spectroscopy results show that the Yb ions carry a spontaneous moment of only $\sim 0.35\ \mu_B$. We think that this small value is mainly a crystal field effect, and that the Kondo coupling, smaller than in $YbNi_2B_2C$, contributes only weakly to the moment reduction. Hybridization however provides an anomalously strong (with respect to other members of the series) and anisotropic RKKY exchange interaction. This leads to a rather high magnetic ordering temperature (4.2 K) and forces the spontaneous moment to lie along a hard magnetisation axis, whence the small spontaneous moment. Therefore, in YbNiBC, opposite and large anisotropies of the electronic g-tensor and of the exchange interaction are at play and govern the low temperature magnetic properties.

In the related system ErNiBC which has a magnetic ordering temperature similar to that of YbNiBC, our ^{166}Er Mössbauer studies show that the moment on Er ions in the ordered state is $\sim 7.7\ \mu_B$ corresponding also to an extremely anisotropic g-tensor. The heat capacity results confirm the bulk magnetic ordering at ~ 4.5 K and corroborate the conclusion derived from Mössbauer data that there are two closely spaced ground crystal field doublets. The Mössbauer spectra in ErNiBC show slow relaxation effects, characterised by the presence of magnetic hyperfine split spectra even above the magnetic transition temperature. This is often observed in Mössbauer spectra of rare earth isotopes when the electronic ground state is extremely anisotropic. This contrasts with the situation in $ErNi_2B_2C$ [18] where, due to an entirely different crystal field ground state, fast electronic fluctuations wipe out the magnetic hyperfine structure above T_N.

Part of this work was carried out under the project 1808-1 of the Indo-French Center for the Promotion of Advanced Research (IFCPAR), New Delhi, India.

References

1. C. Mazumdar, R. Nagarajan, C. Godart, L.C. Gupta, M. Latroche, S.K. Dhar, C. Levy-Clement, B.D. Padalia, R. Vijayaraghavan, Solid State Commun. **87**, 413 (1993).
2. R. Nagarajan, C. Mazumdar, Z. Hossain, S.K. Dhar, K.V. Gopalakrishnan, L.C. Gupta, C. Godart, B.D. Padalia, R. Vijayaraghavan, Phys. Rev. Lett. **72**, 274 (1994).
3. R.J. Cava, H. Takagi, H.W. Zandbergen, J.J. Krajewski, W.F. Peck, T. Siegrist, B. Batlogg, R.B. Van Dover, R.J. Felder, K. Mizuhashi, J.O. Lee, H. Eisaki, S. Uchida, Nature **367**, 252 (1994).
4. H. Eisaki, H. Takagi, R.J. Cava, K. Mizuhashi, J.O. Lee, B. Batlogg, J.J. Krajewski, W.F. Peck Jr., S. Uchida, Phys. Rev. B **50**, 647 (1994).
5. L.C. Gupta, Phil. Mag. **77**, 717 (1998), and references therein.
6. S.K. Dhar, R. Nagarajan, Z. Hossain, E. Tominez, C. Godart, L.C. Gupta, R. Vijayaraghavan, Solid State Commun. **98**, 985 (1996).
7. A. Yatskar, N.K. Budraa, W.P. Beyermann, P.C. Canfield, S.L. Bud'ko, Phys. Rev. B **54**, 3772 (1996).
8. Z. Hossain, R. Nagarajan, S.M. Pattalwar, S.K. Dhar, L.C. Gupta, C. Godart, Physica B **230-232**, 865 (1997).
9. Z. Hossain, R. Nagarajan, S.K. Dhar, L.C. Gupta, J. Magn. Magn. Mater. **184**, 235 (1998).
10. T. Siegrist, H.W. Zandbergen, R.J. Cava, J.J. Krajewski, W.F. Peck, Nature **367**, 254 (1994).
11. M El Massalami, B. Giordarnengo, J. Mondragon, E.M. Baggio-Saitovitch, A. Takeuchi, J. Voiron, A. Sulpice, J. Phys.-Cond. **7**, 10015 (1995).
12. L.J. Chang, C.V. Tomy, D.M^{c}K. Paul, N.H. Andersen, M. Yethiraj, J. Phys.-Cond. **8**, 2119 (1996).
13. A. Amato, Physica B **206-207**, 49 (1995).
14. A. Yaouanc, P. Dalmas de Réotier, A.D. Huxley, P. Bonville, P.C.M. Gubbens, A.M. Mulders, P. Lejay, S. Kunii, Physica **230-232**, 269 (1997).
15. S. Ofer. I. Nowik, S.G. Cohen in *Chemical applications of Mössbauer spectroscopy*, edited by V.I. Goldanski, R.H. Herber (Academic Press, 1968), p. 428.
16. P. Bonville, P. Bellot, J.A. Hodges, P. Imbert, G. Jéhanno, G. LeBras, J. Hammann, L. Leylekian, G. Chevrier, P. Thuéry, L. D'Onofrio, A. Hamzic, A. Barthélémy, Physica B **182**, 105 (1992).
17. A. Abragam, B. Bleaney, *Electron paramagnetic resonance of transition ions* (Clarendon Press, Oxford, 1970).
18. P. Bonville, J.A. Hodges, C. Vaast, E. Alleno, C. Godart, L.C. Gupta, Z.Hossain, R. Nagarajan, G. Hilscher, H. Michor, Z. Phys. B **101**, 511 (1996).
19. I. Nowik, Phys. Lett. **15**, 219 (1965).
20. S. Doniach, Physica B **91**, 231 (1977).
21. L.C. Gupta, D.E. MacLaughlin, Cheng Tien, C. Godart, M.A. Edwards, R.D. Parks, Phys. Rev. B **28**, 3673 (1983).
22. P. Bonville, E. Vincent, E. Bauer, Eur. Phys. J. B **8**, 363 (1999).